ADCT-301, a Pyrrolobenzodiazepine (PBD) Dimer-Containing Antibody Drug Conjugate (ADC) Targeting CD25-Expressing Hematological Malignancies

Michael J Flynn[1,2], Francesca Zammarchi[3], Peter C Tyrer[2], Ayse U Akarca[4], Narinder Janghra[4], Charles E Britten[3], Carin EG Havenith[3], Jean-Noel Levy[2], Arnaud Tiberghien[2], Luke A Masterson[2], Conor Barry[2], Francois D'Hooge[2], Teresa Marafioti[4], Paul WHI Parren[5,6], David G Williams[2], Philip W Howard[2], Patrick H van Berkel[3] and John A Hartley[1,2]

[1]Cancer Research UK Drug DNA Interactions Research Group, UCL Cancer Institute, 72 Huntley Street, London, WC1E 6BT, UK

[2]Spirogen Ltd, QMB Innovation Centre, 42 New Road, London, E1 2AX, UK

[3]ADC Therapeutics (UK) limited, QMB Innovation Centre, 42 New Road, London, E1 2AX, UK

[4]Department of Pathology, University College London, London, WC1E 6BT, UK

[5]Genmab, Yalelaan 60, 3584 CX Utrecht, the Netherlands

[6]Department of Immunohematology and Blood Transfusion, Leiden University Medical Center, Albinusdreef 2, 2333 ZA, Leiden, the Netherlands

Running title: ADCT-301 targets CD25-expressing hematological malignancies

Conflict-of-interest disclosure: M.J. Flynn, P.C. Tyrer, D.G. Williams, P.W. Howard and J.A. Hartley are employees of Spirogen/Medimmune limited. P.H van Berkel, F. Zammarchi, C.E. Britten and C.G. Havenith are employees of ADC Therapeutics and P.H. van Berkel, J.A. Hartley and P.W. Howard are also major shareholders. P.W.H.I. Parren is an employee of Genmab. J.A. Hartley acknowledges Programme Grant support from Cancer Research UK (C2559A/A16569).

Abstract

Despite the many advances in the treatment of hematological malignancies over the past decade, outcomes in refractory lymphomas remain poor. One potential strategy in this patient population is the specific targeting of IL-2R-α (CD25), which is over-expressed on many lymphoma and leukemic cells, using antibody drug conjugates (ADCs). ADCT-301 is an ADC composed of human IgG1 HuMax®-TAC against CD25, stochastically conjugated through a dipeptide cleavable linker to a pyrrolobenzodiazepine (PBD) dimer warhead with a drug-antibody ratio (DAR) of 2.3. ADCT-301 binds human CD25 with picomolar affinity. ADCT-301 has highly potent and selective cytotoxicity against a panel of CD25-expressing human lymphoma cell lines. Once internalized, the released warhead binds in the DNA minor groove and exerts its potent cytotoxic action via the formation of DNA interstrand cross-links. A strong correlation between loss of viability and DNA cross-link formation is demonstrated. DNA damage persists, resulting in phosphorylation of histone H2AX, cell cycle arrest in G2/M and apoptosis. Bystander killing of CD25-negative cells by ADCT-301 is also observed. *In vivo*, a single-dose of ADCT-301 results in dose-dependent and targeted antitumor activity against both subcutaneous and disseminated CD25-positive lymphoma models. In xenografts of Karpas 299, which expressed both CD25 and CD30, marked superiority over brentuximab vedotin (Adcetris®) is observed. Dose-dependent increases in DNA cross-linking, γ-H2AX and PBD payload staining were observed in tumors *in vivo* indicating a role as relevant pharmacodynamic assays. Together these data support the clinical testing of this novel ADC in patients with CD25-expressing tumors.

Introduction

In 2015 in the United States there were an estimated 80,900 and 54,270 new diagnoses of all-type lymphoma and leukemia, and 20,490 and 24,450 deaths, respectively.(1) Both Hodgkin's lymphoma (HL) and various T and B-cell Non-Hodgkin's lymphoma (NHL) tumor cells express IL-2R-α (CD25).(2, 3) At least two leukemic diseases, Adult T-cell leukemia lymphoma (ATLL)(4) and hairy cell leukemia(5), show near 100% expression of CD25 on their circulating tumor cells. In the refractory setting there is evidence of maintenance of CD25 expression, and in acute myeloid leukemia (AML), its upregulation.(6) Although not unique to hematological malignancy, increased CD25 expression can be detected via shedding of this receptor.(7, 8) Indeed, high soluble IL-2R-α serum levels have helped identify patients with poorer prognoses in diffuse large B-cell lymphoma, cutaneous lymphomas, follicular lymphoma, AML, acute lymphoblastic leukemia, Hodgkin's lymphoma(9-14) and are used as part of a prognostic index in ATLL.(15)

A number of clinical trials have, demonstrated the utility of targeting this receptor in oncology. Phase I clinical trials of three radioimmunoconjugates, ^{90}Yttrium-labeled anti-Tac(16),^{131}Iodine-labeled basiliximab(17) and ^{90}Yttrium-labeled daclizumab(18) have demonstrated complete responses in patients with CD25-expressing lymphomas. The delayed myelosuppression seen with each of these anti-CD25 radionuclides was thought to be due to each β-emitting radionuclide having an effect on red marrow rather than an anti-CD25 antibody specific effect (16-18). Two anti-CD25 immunotoxin conjugates have been tested in a number of human trials. LMB-2, a pseudomonal exotoxin conjugated to an anti-CD25 single chain variable fragment (19) has shown objective responses in CD25-expressing lymphomas including ATLL(20) and denileukin-diftitox (Ontak™), a diphtheria exotoxin conjugated to an IL-2 fragment(21) is licensed in CD25-positive cutaneous T cell lymphoma. Despite immunogenicity and manufacturing obstacles (22), immunotoxins remain a promising field of targeted therapies. (23) Anti-CD25 radioimmunoconjugates and

immunotoxins have both provided proof of concept for the feasibility of targeting the CD25 receptor with few toxicity concerns and have provided a platform for the preclinical development of new anti-CD25 targeting drugs.

The development of ADCs, however, has arguably been the immunoconjugate class most propelled by the commercial successes of therapeutic monoclonal antibody technologies. (24) This is at least partly because the synthesis of purified ADCs can now be carried out in a controlled way using optimised linker technologies. (24) The use of antibody drug conjugates (ADCs) in oncology indications has risen to prominence in the past decade, highlighted by FDA licensing of Adcetris in 2011 and trastuzumab emtansine (Kadcyla ®) in 2013.(24) More recently novel ADCs delivering pyrrolobenzodiazepine (PBD) dimers as the cytotoxic warhead have been developed. PBD dimers are a class of exquisitely-potent DNA minor groove interstrand cross-linking agents, one of which, SG2000 (SJG-136), has shown activity against both solid tumors and hematological malignancies.(25, 26) Advantages over ADCs targeting other warheads including tubulin inhibitors (e.g. auristatins and maytansinoids), DNA damaging drugs (e.g. calicheamicin) and classical chemotherapeutics include the ability to target low copy number antigens, and to exploit low drug antibody ratios (DARs). Due to their novel mechanism of action, PBD-containing ADCs are active in tumors inherently resistant to other warhead types and against multidrug resistant tumors.(27)

Here we report the characterization, mechanism of action and preclinical evaluation of a novel anti-CD25 ADC, ADCT-301.

Materials and methods

Synthesis of ADCT-301

HuMax-TAC antibody was first buffer exchanged into a proprietary histidine buffer at pH 6 containing various carbohydrate-based stabilising additives using tangential flow filtration (TFF) on Pellicon 30kDa cassettes using 10 diavolumes at constant TMP of 1.0 bar. Antibody was concentrated to ca. 10 mg/ml and the pH was adjusted to 7.5 using a TRIS/EDTA ph 8.5 buffer. 10mM TCEP reductant was added to the batch as a 1.25 excess with respect to HuMax-TAC mAb and the reduction reaction was allowed to proceed for 60 min at 20˚C. Dimethylacetamide (DMA) and 10 mM SG3249 (28) were added to the solution to a final 5% DMA v/v and three-fold excess relative to antibody. The conjugation reaction was incubated at 20 ˚C for 60 min, then quenched with three-fold molar excess of N-Acetyl cysteine and incubated at 20˚C for 20 min. The pH was then decreased to 6.0 using histidine hydrochloride solution and the ADC purified by TFF using the same conditions as the first buffer exchange step, this time with 12 diavolumes of the histidine/carbohydrate additive buffer. The solution was filtered (0.22 µm) and stored at -70°C. Final yield was estimated from starting antibody by UV/Vis.

Human cell lines

The anaplastic large cell lymphoma (ALCL) cell lines Karpas 299 (2012) and Su-DHL-1 (2012) and the Hodgkin's lymphoma (HL) cell lines L-540 (2014) and HDLM-2 (2014) were obtained from the Deutsche Sammlung von Mikroorganismen und Zellkuturen (DSMZ) (Braunschweig, Germany). The Burkitt lymphoma cell lines Daudi (2012) and Ramos (2012) and the cutaneous T-cell lymphoma line HuT-78 (2013) were obtained from the American Type Culture Collection (ATCC) supplier LGC Standards (Middlesex, UK). The myeloid leukemia cell lines, EoL-1 and KG-1 were obtained from DSMZ and LGC Standards, respectively (2015). Characterization of these mycoplasma negative cell lines was

performed by the cell bank supplier and included the determination and the verification of tissue-specific antibodies, karyotyping and expression of aberrantly expressed genes. As cell lines were passaged for fewer than 6 months after receipt or resuscitation, they were not authenticated or tested in our laboratory. Cells were cultured in RPMI-1640 media (Sigma-Aldrich, Dorset, UK) or IMDM (LGC Standards) with added *L*-glutamine (Sigma-Aldrich) or in *L*-glutamine-containing media (LifeTech, Paisley, UK) each of which was supplemented with heat-inactivated fetal bovine serum (FBS) as per the supplier's instructions.

In vitro binding and internalization assays

Binding of HuMax-TAC or ADCT-301 to cell lines was detected with an Alexa Fluor 488 (AF488)-labeled anti-human IgG (LifeTech). For internalization studies, Karpas 299 cells were exposed (1h at 4°C) to ADCT-301 in blocking buffer (PBS, 10% (v/v) normal goat serum, 0.1% sodium azide (w/v)). Cells were washed and incubated for various periods in medium over a time course at 37°C after which time they were centrifuged, washed and fixed (neutral buffered formalin). Once all time points were collected, plates were centrifuged (400 *g*), washed and incubated with either a saturating antibody concentration of mouse IgG1 CD25 antibody (BD Biosciences) or a mouse non-targeted (isotype control) monoclonal antibody MOPC (BD Biosciences), in blocking buffer for 1h at 4°C. The potential for competition of binding to the same IL-2R-α epitope by ADCT-301 and mouse anti-human CD25 was measured in a competition assay by co-incubation of cells with increasing concentrations of ADCT-301 and a saturating concentration of mouse anti-human CD25. After washing and re-suspension, the Qifikit protocol(29) (DAKO, Cambridge, UK) was followed, labeling cells with an anti-mouse FITC-labeled antibody (DAKO). For immunofluorescent imaging of ADCT-301 treated CD25-positive cell lines, cells were fixed (4% paraformaldehyde) at each time point, re-suspended in permeabilization/wash buffer (BD Biosciences) and then incubated with APC-labeled mouse anti-human LAMP-1 (BD Biosciences) and AF488-labeled anti-human antibody (LifeTech), while nuclear counterstaining was performed with Hoechst 33342 (LifeTech) (1h at 4°C). After cell

cytospins were generated, slides were mounted with prolong gold antifade (LifeTech) and slide edges sealed with clear nail polish. Images from dried slides kept at 4°C were captured on a TCS SPE confocal system utilizing a DM2500 microscope (Leica) (40x or 63x oil immersion objective) using three solid state excitation lasers (405, 488 and 635 nm). Alternatively, Karpas 299 cells were incubated with ADCT-301, washed, and then either kept at 4°C in PBS, 0.1% azide or re-suspended in medium and incubated at 37°C over a time course to 4h. After each time point, cells were washed and incubated with an AF488-labeled anti-human IgG (1h at 4°C). After washing and re-suspension of all labeled cells in PBS, 0.1% sodium azide, cells were analyzed on an Accuri, C6 flow cytometer (BD Biosciences, Oxford, UK). Median fluorescent intensity (MFI) of the live cell population was determined using Flowjo 7.0 (Tree Star Inc., Ashland, OR). GraphPad (San Diego, CA) was used to calculate an EC_{50} or a linear regression model for calculating CD25 molecule numbers per cell. The Qifikit protocol(29) was also used to determine CD30 copy number with a mouse IgG1 CD30 antibody (GeneTex, Nottingham, UK).

Surface plasmon resonance

Human soluble CD25-streptavidin fusion protein transiently produced in CHO cells (Evitria, Zurich, Switzerland) was immobilised by amine coupling to a Biacore CM3 sensor chip (GE Healthcare, Little Chalfont, UK). A concentration range (0.05 to 5 nM) of HuMax-TAC and ADCT-301 was injected over the chip for 120 seconds as per the Biacore multi-cycle kinetics method and allowed to dissociate by running HBS-EP buffer (Hepes-buffered saline containing EDTA and surfactant P20) over the chip for 60min. The equilibrium dissociation constant K_D was calculated with Biaevaluation software (GE).

Cell survival determination by MTS assay

Cell viability was measured following either 96h incubation at 37°C to ADC, non-binding ADC or warhead dilution series, or a 2h exposure and wash, followed by further 94h incubation. For the measurement of bystander killing, Karpas 299 cells were incubated with

serial dilutions of ADCT-301 or non-binding ADC in 96-well round-bottom plates for 48h. Centrifuged Karpas 299 conditioned medium (50 µl) was added to 50 µl of Ramos cell culture in 96-well flat-bottom plates and incubated for 96h. For all experiments cell survival was determined by absorbance measurements on a Varioskan™ Flash Multimode Reader (Thermo Fisher Scientific, Hempstead, UK) according to a standard MTS protocol.(30) Percentage growth inhibition was calculated from the mean absorbance in the triplicate ADC-treated wells, compared to the mean absorbance in the control wells (100 %). Dose-response curves were generated from the mean data of each independent experiment. The GI_{50} was determined by fitting a sigmoidal dose response curve to the data using Graphpad.

Co-culture and viability flow cytometry assays

Unlabeled Karpas 299 cells and PKH-26-labeled (Sigma-Aldrich, UK) Ramos cells (20 µM) were diluted (1.5×10^5 cells/ml) in medium and dispensed into round-bottom, ultralow-attachment 96-well microplates (Corning) as follows: mono-culture: 50 µl cells plus 50 µl growth medium; co-cultures: 50µl Karpas 299 plus 50 µl labeled Ramos. Serial dilutions of ADCT-301 and non-binding ADC, containing 20 µM TGF-β inhibitor, SB431542 (Sigma-Aldrich) were added (100µl/well) to single and co-cultures. Cells were mixed on an IKA Vibrax shaker (10sec) and incubated at 37°C for 96h. After washing and re-suspension in PBS, Fixable Dead Cell Stain (LifeTech) was added. Cells were re-suspended and incubated in the dark for 30 min. Alternatively, in apoptosis experiments, Karpas 299 cells (1.5×10^5/ml) were dispensed with ADCT-301 or non-binding ADC as described above. Etoposide was used as a positive apoptosis control. Cells were incubated at 37°C over a time course. At each time point, cells were centrifuged, washed, re-suspended in Fixable Dead Cell Stain and FITC-labeled Annexin-V antibody (BD Biosciences) diluted in Annexin-V Calcium free buffer and incubated for 30min (RT). Annexin-V buffer (250µl) was added to each well before analysis on an Accuri C6 flow cytometer. Data were analyzed in FlowJo. Total, live and dead cell counts from three replicate experiments were obtained from quadrant plots after compensation was carried out as necessary. Counts were normalised to

the total cell count per well for each condition, to reflect the percentage of cells that remained viable or were apoptosed.

In vitro and *in vivo* cross-linking determination by single cell gel electrophoresis (comet) assay

Cell lines were incubated with ADCT-301 or non-binding ADC (20 ng/ml) for 2h at 37°C, washed, re-suspended in medium and incubated at 37°C over a further time course (2 - 36h). After each time point, cells were centrifuged, re-suspended in freezing medium (FBS with 10% DMSO) and frozen at -80°C. An equimolar concentration of SG3199 was dispensed into cell suspension, incubated for two hours and the same procedure for harvesting ADC-exposed cells followed. To determine percentage cross-linking of increasing doses of ADCT-301 or non-binding ADC on expressing cell lines each ADC dilution was added to cells for two hours at 37°C. Cells were washed, re-suspended in culture medium, dispensed into 24 well plates, incubated for 24h at 37°C and harvested, as above. For analysis of cross-linking on Karpas 299 subcutaneously implanted into SCID mice, cell suspensions were prepared from the excised tumors removed 24h after dosing with 0.2 or 0.6 mg/kg ADCT-301 or left untreated and stored in freezing medium at -80°C. Peripheral blood mononuclear cells (PBMCs) from each mouse were isolated from whole blood using a Ficoll gradient and stored in freezing medium at -80°C. Frozen cells were thawed on ice, re-suspended in cold RPMI (Sigma) and counted. Cell suspensions (2-3 x 10^4 cells/ml), excepting un-irradiated controls, were irradiated (15 Gy) and kept on ice. The Comet assay was performed as previously described.(31) Slides were reviewed under a 20x objective on an epi-fluorescence microscope equipped with: Hg arc lamp; 580 nm dichroic mirror; and 535 nm excitation and 645 nm emission filters suitable for visualising propidium iodide staining with a minimum of 50 Comet images acquired per treatment condition. The Olive Tail Moment (OTM) was determined as the product of the tail length and the fraction of total DNA in the tail as recorded by Komet 6 software (Andor Technology, Belfast, UK) and the percentage reduction in OTM calculated according to the formula:

$$\% \text{ decrease in tail moment} = [1- (TMdi- TMcu)/(TMci – TMcu)] * 100$$

TMdi= Tail Moment drug irradiated; TMcu= TM control un-irradiated; TMci = TM control irradiated

Analysis was performed on Microsoft Excel and GraphPad.

γ-H2AX foci quantification

Karpas 299 cells treated with serial dilutions of ADCT-301 concentrations and frozen at -80°C, were thawed, washed in PBS, fixed with 4% paraformaldehyde for 5min at room temperature and washed in PBS. Cell cytospins were generated for each treatment condition and cells were permeabilized with PBS/0.2% Triton-X100, washed in PBS and blocked in 10% FBS, 5% BSA in PBS. After incubation overnight (4°C) with goat anti-mouse γ-H2AX (JBW301) (Millipore, UK) in 1% FBS in PBS, slides were washed and incubated (1h at RT) with AF488-labeled goat anti-mouse IgG antibody (LifeTech) then counterstained with Hoecsht 33342 (LifeTech). Slides were washed in PBS and distilled water, mounted with prolong gold antifade (LifeTech) and the coverslip edges sealed with clear nail polish. Images captured on a confocal system as described above, were compressed to a maximum intensity projection image of z-stack acquired images to allow maximal detection of foci and analyzed in Image J. Cell Profiler was used to quantify γ-H2AX foci per cell in at least 20 cells per treatment.

Cell cycle analysis

Karpas 299 cells were treated with ADCT-301, SG3199, non-binding ADC or left untreated. Ethanol fixed nuclei were stained with 0.5 mg/ml propidium iodide (PI) (Sigma) in the presence of 100 µg/ml RNAase (Sigma) (1h at 37°C). Cells were analyzed by flow cytometry (FACSVerse, BD Bioscience). Histograms of the singlet live cell population in the PI emission spectrum were drawn using the cell cycle function in Flowjo and analyses of cell cycle percentages performed in GraphPad.

Assessment of ADCT-301 efficacy in subcutaneous *in vivo* models

Karpas 299 xenografts were established in 6-8 week old female Fox Chase SCID® (C.B-17/Icr-*Prkdcscid*, Charles River) by implanting 10^7 cells subcutaneously into their flanks. Su-DHL-1 xenografts were established by injection of 10^7 cells (50% matrigel) into 10 week old nude mice (Nu (NCr)-Fox1nu, Charles River). When tumors reached approximately 100-155 mm^3 mice were randomly allocated into groups to receive ADCT-301, non-binding ADC, PBS (vehicle) or Adcetris intravenously. Clinical grade Adcetris was purchased from Seattle Genetics (Seattle, WA). Mice were in the body weight range of 15.5 to 27.6 g on Day 1 of the studies. Each animal was euthanized when its tumor reached the endpoint volume of 2,000 mm^3 or at study end. The time to endpoint (TTE) for analysis was calculated for each mouse by the following equation:

$$\text{TTE (days)} = ([\log_{10}(\text{endpoint volume} - \text{intercept*}] / \text{slope*})$$

*of the line obtained by linear regression of a log-transformed tumor growth data set

The logrank test was used to analyze the significance of differences between the TTE values of two groups. The setup of experimental procedures used in Karpas 299 and Ramos disseminated models are described in Supplemental Methods and Tables.

Assessment of ADCT-301 pharmacokinetics and toxicity in non-tumor bearing SCID mice

ADCT-301 was administered i.v. as a single dose (1-12 mg/kg) to non-tumor bearing CB.17 SCID mice, following which mice were observed for weight changes and toxicities. Alternatively, to measure the pharmacokinetic profile of naked antibody, HuMax-Tac or ADCT-301, 1 mg/kg of each drug was administered i.v as a single dose to non-tumor bearing mice. Blood collection was performed at specified time points (25 µL of blood from mice tail veins diluted in 225 µL PBS in 6% EDTA). The samples were spun down at 400 *g* for 5 mins, the supernatant was aspirated and stored at -80°C and measurement of samples'

total antibody and ADC (DAR ≥ 1) concentrations performed by an optimised ELISA assay. In order to measure antibody in each sample, Immuno MaxiSorp plates (Thermo Fisher Scientific) were first coated with sCD25-Strepavidin (Evitria) in PBS and incubated overnight (4°C). Alternatively, to measure conjugated ADC, DAR >=1, identical plates were coated with anti-PBD antibody in PBS and incubated overnight (4°C). Plates were then washed x 3 (0.05% Tween) and blocked (3% BSA/PBS) for 1h. Reference, QC and test samples were prepared and added to polypropylene plates (Thermo Fisher Scientific) (2 h at RT). They were then washed x 3 and mouse anti-human IgG1-HRP conjugate (Sanquin) added and plates incubated for 1h (RT). Plates were washed x 3, Ultra TMB (Thermo Fisher Scientific) added and incubated for 10 min at RT. Stop solution of 1M HCL was added and absorbance was read at 450 nm on an Envision plate reader. In order to quantify absorbance, calibration curves were established in assay buffer (0.5xBlotto+0.05% Tween in PBS) containing 2.5% or 0.5% pooled mouse serum. The pharmacokinetic analysis of ADCT-301 and HuMax-TAC concentrations was performed using Phoenix WinNonlin Version 6.2 with non-compartmental analysis.

Animal care compliance

The Institutional Animal Care and Use Program at Charles River Discovery Services are accredited by the Association for Assessment and Accreditation of Laboratory Animal Care International (AAALAC), which assures compliance with accepted standards for the care and use of laboratory animals.

Immunohistochemistry of tumor xenograft sections

Murine xenograft tumors untreated or treated with 0.2 mg/kg or 0.6 mg/kg ADCT-301 were fixed in buffered formalin and embedded in paraffin according to a conventional protocol. 2-5 µm sections were cut and transferred on electrically charged slides to be subjected to immunohistochemistry. Testing of an anti-SG3249 payload antibody (14B3-B7) (ADC Therapeutics, UK) and an antibody to detect phosphorylation of Histone H2A.X at position

Ser139 (New England Biolabs, Hitchin, UK) was carried out with staining conditions (i.e. antibody dilution, incubation time, and antigen retrieval method) optimized on ADCT-301-treated or irradiated-Karpas 299 cytospins. Single immunostaining was performed using a BOND-III Autostainer (Leica Microsystems, UK) according to protocols described elsewhere.(32, 33) Stained slides were scanned with the NanoZoomer Digital Pathology System (Hamamatsu, Japan) and images reviewed with NDP viewer.

Results

Properties of ADCT-301

ADCT-301 is an ADC composed of HuMax®-TAC, a human IgG1 anti-CD25 antibody, maleimide-conjugated at reduced interchain cysteines via a cathepsin-cleavable valine-alanine (val-ala) linker to PBD dimer warhead SG3199 (Figure 1A). The ADC was 97% monodisperse as determined by size-exclusion chromatography (Supplemental Figure S1A, Supplemental Table S1). Drug antibody ratio (DAR) was determined by reverse-phase liquid chromotography to be 2.25 (Supplemental Figure S1B, Supplemental Table S2) and by hydrophobic interaction chromatography to be 2.19 (Supplemental Figure S1C, Supplemental Table S3).

HuMax-TAC and ADCT-301 showed strong binding affinity to CD25-positive human anaplastic large cell lymphoma derived cell lines Karpas 299 and Su-DHL-1 (Figure 1B). Estimated EC_{50s} were in the sub-nanomolar range and were marginally lower for HuMax-TAC than ADCT-301 in both lines. Binding saturated at around 1 µg/ml for both cell lines, but the MFI was approximately three-fold higher in the Su-DHL-1 compared to the Karpas 299 cell line reflecting the difference in copy number (Table 1). In contrast, a non-binding ADC containing the same drug linker payload showed no binding to either cell line at 30 µg/ml. Using soluble CD25 ectodomain, equilibrium dissociation constant (K_D) measurements of HuMax-TAC or ADCT-301 determined by surface plasmon resonance were 15 pM and 20 pM, respectively. Representative SPR sensorgrams for HuMax-TAC and ADCT-301 are shown in Figure 1C and 1D, respectively.

Selective cytotoxicity of ADCT-301 *in vitro*

The *in vitro* cytotoxicity of ADCT-301 was determined in a panel of human lymphoma CD25-expressing (Su-DHL-1, HDLM-2, L540, Karpas 299) and non-expressing (Ramos, HuT-78, Daudi) cell lines. These values were derived from graphs shown in Supplemental Figure S2A. Additionally, cytotoxicity in myeloid leukemia lines, EoL-1 (CD25-expressing) and KG-1

(CD25 non-expressing) was determined. As shown in Table 1, the GI_{50} values for ADCT-301 in the CD25-positive lines ranged from 0.04-2.94 ng/ml. GI_{50} values in the CD25-negative lines were > 1,000 ng/ml. The non-binding ADC gave GI_{50} values > 1,000 ng/ml in both antigen expressing and non-expressing lines (Supplemental Figure S2B). No clear relationship between GI_{50} value and mean CD25 copy number was observed for ADCT-301 in the five CD25-positive cell lines ($r=-0.07$; $p = 0.91$). In contrast to the ADC, the naked warhead, SG3199, was cytotoxic against all the lines tested and did not discriminate between CD25-expressing and non-expressing cells (Table 1). HuMax-TAC antibody up to 1,000 ng/ml was not cytotoxic in CD25-positive or CD25-negative cell lines (Supplemental Figure S2C).

Following exposure to ADCT-301, reduction of CD25-negative Ramos cell viability was shown when co-cultured (50:50) with CD25-expressing Karpas 299 cells, indicating a bystander killing effect (Figure 2A upper panel). ADCT-301 at both 1 and 10 ng/ml induced a highly significant difference ($p \leq 0.001$) in Ramos viability in mono-culture compared to Ramos+Karpas 299 co-culture. A significant difference ($p \leq 0.05$) between GI_{50} values for Ramos treated for 96h with the medium taken from 48h ADCT-301-treated Karpas 299 and Ramos treated for 96h with ADCT-301 in fresh medium was also demonstrated (Figure 2B upper panel). In contrast, there was no significant effect on Ramos survival when treated with 1 or 10 ng/ml of non-binding ADC (Figure 2A lower panel) or conditioned media taken from non-binding ADC-treated Karpas 299 (Figure 2B lower panel).

ADCT-301 internalization

CD25-expressing cells exposed to ADCT-301 (1h at 4°C) showed prominent cell surface binding (T=0h) (Figure 2C). On incubation at 37°C, ADCT-301 is beginning to be internalized by 1h with cell membrane labelling still evident and co-localization with lysosomes observed by 4h. In contrast, no cell surface binding is observed with a non-binding ADC at T=0h. For Karpas 299, there was a reduction of CD25 molecules on the cell surface, as measured by a

reduction in MFI of cells labeled with a FITC-conjugated non-competitive anti-CD25 antibody, over the first three hours post-treatment. The change in surface CD25 molecules after ADCT-301 exposure was significant ($p \leq 0.05$) compared to that observed after non-binding ADC exposure. A return to pre-treatment CD25 MFI occurred by 16h (Figure 2D). In addition to a change in CD25 receptor number, the MFI of cells incubated with ADCT-301 and stained with an AF488-labeled anti-human IgG antibody was reduced over a time course up to 4h following incubation at 37°C (Figure 2E).

DNA interstrand cross-link formation

DNA interstrand cross-linking was measured using a modification of the single cell gel electrophoresis (comet) assay. Representative comet images are shown in Figure 3A. Cross-linking was expressed as the percentage decrease in the Olive Tail Moment (OTM) compared to control irradiated cells. Following a two-hour exposure of Karpas 299 cells to 20 ng/ml of ADCT-301, the time course of cross-link formation is shown in Figure 3B. Cross-links formed after an initial delay, reaching a peak between four and eight hours. In contrast, the free warhead at an equimolar equivalent warhead dose reached the peak of cross-linking during the two hour exposure. In both cases cross-links persisted over at least 36 hours. The non-binding ADC at 20 ng/ml did not show a significant reduction in OTM over the same time course. An equivalent experiment in Su-DHL-1 cells, gave the same kinetics of cross-link formation resulting in a slightly higher peak (Figure 3C), possibly reflecting the higher CD25 copy number and sensitivity of this line to ADCT-301.

At maximum cross-linking (24h) in both Karpas 299 (Figure 3D) and Su-DHL-1 (Figure 3E), a correlation between loss of viability and cross-link formation ($r = 0.9745$ and $r = 0.9485$, respectively; $p \leq 0.05$) was established. No evidence of cross-linking after treatment with 1 µg/ml ADCT-301 could be demonstrated in CD25-negative Daudi cells (Supplemental Figure S3). However, cross-linking by naked warhead in CD25-negative Daudi was similar to that in CD25-positive cell lines.

DNA damage response, cell cycle arrest and apoptosis

We have previously shown that PBD-induced DNA interstrand cross-links induce a robust, but delayed γ- H2AX response (34). In Karpas 299 cells γ-H2AX foci were observed 24h after a two-hour exposure to sub-GI_{50} concentrations of ADCT-301 (Figure 4A). After treatment with 60 pg/ml or 1000 pg/ml ADCT-301, γ-H2AX foci increased by 17 or 34 fold relative to untreated cells, respectively ($p \leq 0.05$ and $p \leq 0.01$). In these cells continuous exposure to 3 or 10 ng/ml ADCT-301 resulted in a dose-dependent G2/M arrest reaching a maximum at 48h as evidenced by a decreased percentage of cells in G0/G1 and an increased percentage in G2/M compared to untreated control (Figure 4B). A GI_{50} warhead concentration (15 pM) induced G2/M cell cycle arrest in a similar fashion to a GI_{50} concentration of ADCT-301 (3 ng/ml - containing the equivalent of 46 pM of payload in this cell line, although this occurred earlier peaking at 24h (Figure 4C). After continuous exposure to 10 ng/ml ADCT-301, the peak of the early apoptosis marker annexin-V on the cell surface of Karpas 299 cells was observed between 60 and 72h (Figure 4D). Maximal loss of viability was at 96h. Non-binding ADC (10 ng/ml) did not induce cell cycle G2/M arrest (Figure 4B) or increased Annexin-V and loss of viability (Figure 4D).

***In vivo* efficacy of ADCT-301**

In vivo, ADCT-301 demonstrated dose-dependent antitumor activity against both subcutaneous and disseminated lymphoma models. In the subcutaneous CD25-expressing Karpas 299 xenograft, a single dose of ADCT-301 delayed tumor growth in a dose-dependent fashion with the 0.6 mg/kg cohort demonstrating 10/10 tumor-free survivors at Day 60 (Figure 5A). TTE survival analyses compared to vehicle control were superior at 0.1 mg/kg (log-rank test $p \leq 0.05$) and at 0.2, 0.4 and 0.6 mg/kg ($p \leq 0.001$) (Supplemental Figure S4A). Similarly a single dose of 0.5 mg/kg ADCT-301 produced 10/10 tumor-free survivors maintained at Day 75, whereas a single dose of 0.5 mg/kg Adcetris (targeting CD30) only delayed tumor growth and even four 0.5 mg/kg doses (q4d x 4) failed to cure

mice (Figure 5B). CD30 expression on Karpas 299 is two to three times higher than CD25 (inset to Figure 5B). Kaplan Meier analyses showed ADCT-301 significantly superior ($p \leq 0.01$) to Adcetris single dose administration (Supplemental Figure S4B). In a disseminated Karpas 299 model, single dose ADCT-301 also showed significant dose-dependent extensions of survival in comparison to vehicle control at all four doses tested ($p \leq 0.001$) (Supplemental Figure S5A). Single-dose ADCT-301 at 0.6 mg/kg showed significant ($p \leq 0.05$) improvement in survival compared to single-dose Adcetris administration (Supplemental Figure S5B). In both subcutaneous and disseminated models (0.5 mg/kg and 0.6 mg/kg, respectively) non-binding ADC failed to show significant tumor regression or survival benefit compared to vehicle controls (Figure 5B, Supplemental Figure S4B, Supplemental Figure S5A). In the subcutaneous Su-DHL-1 xenograft, a single dose of ADCT-301 delayed tumor growth in a dose-dependent fashion with the 0.6 mg/kg cohort demonstrating 6/8 tumor-free survivors at Day 74 (Figure 5C). In contrast, single dose (0.5 mg/kg) ADCT-301 in disseminated CD25-negative Ramos xenografts failed to show a survival benefit (Supplemental Figure S6). In non-tumor bearing SCID mice the maximum tolerated dose, as defined by less than 10% weight loss, was 9 mg/kg ADCT-301. The half-life of naked antibody, HuMax-Tac was 7.3 days. Similarly, the half-life of ADCT-301 by analysis of the conjugated antibody with DAR component ≥ 1 was 7.3 days.

Pharmacodynamic assessment of ADCT-301 *in vivo*

In SCID mice with Karpas 299 subcutaneous tumors, a single dose of ADCT-301 was administered at 0.2 or 0.6 mg/kg. 24h after treatment, excised tumors showed a dose related increase in intensity of staining by an anti-PBD payload antibody and a γ-H2AX antibody (Figure 5D). A magnified section of the ADCT-301 0.6 mg/kg anti-PBD payload antibody panel indicates that tumour cells demonstrate both membrane and cytosolic staining. Reduction in OTM was 23% (0.2 mg/kg) vs 49% (0.6 mg/kg) ($p \leq 0.01$) using the comet assay (Figure 5E). No cross-linking was observed in peripheral blood lymphocyte samples from the same mice (Supplemental Figure S7). The selective targeting of ADCT-301 to

CD25-expressing tumor cells and resulting formation of DNA interstrand cross-links and associated DNA damage response are therefore confirmed *in vivo*.

Discussion

ADCs delivering PBD dimer payloads represent a novel mode of action in the ADC arena. They exploit a completely different cellular mechanism to the widely used auristatin and maytansinoid tubulin inhibitors and a different mode of action to other DNA-interacting warheads such as calicheamicin.(27) Several PBD-containing ADCs are now in Phase I clinical trials including SGN-33A(27), SGN-70A(35), SC16LD6.5(36) and ADCT-301. In the synthesis of ADCT-301, the warhead SG3199 is connected via its N10 position to a maleimidocaproyl val-ala dipeptide linker (as in SC16LD6.5). The maleimide then covalently and stochastically reacts with a limited number of reduced inter-chain disulphide bonds in HuMax-TAC. In contrast, SGN-33A and SGN-70A are conjugated via a val-ala linker to the C2 position on the PBD dimer SGD-1882. Since the N10 position imine is involved in covalent binding to DNA, linker attachment at this point produces a pro-drug and an ADC payload as well as potentially adding a further level of safety. As a result, attachment at the N10 imine requires a self-immolative linker that becomes completely traceless following cleavage.

Binding of ADCT-301 and HuMax-TAC to CD25-positive cell lines (flow cytometry) and to soluble CD25 (SPR) was comparable, indicating that conjugation to PBD-linker did not affect antigen binding. Our *in vitro* models show that HuMax-TAC is not itself directly cytotoxic. All cell lines studied were sensitive to SG3199 warhead. The CD25-positive cell line least sensitive to ADCT-301 was also least sensitive to SG3199 warhead. In all four CD25-positive lymphoma cell lines tested picomolar potency to ADCT-301 is demonstrated but there was no clear relation between sensitivity to ADCT-301 and CD25 expression level. All these cells lines however had high levels of CD25 expression (77,000 to 310,000) and cell lines with much lower CD25 expression may be required to determine the threshold for cytotoxic sensitivity. An eosinophilic leukemia cell line, EoL-1 with a surface CD25 expression of 17,000 demonstrated femtomolar *in vitro* sensitivity to ADCT-301 and free SG3199, suggesting that tumor type sensitivity to free warhead varies considerably between

tumor types and may predict targeted ADC cytotoxicity independently of CD25 expression level above a certain threshold expression level.

If ADCT-301 is to be efficacious in lymphomas with heterogeneous CD25 expression(2), the existence of bystander toxicity on target-negative tumor cells is important. PBD warhead released from the target-positive cell would be expected to be diffusible in contrast to less permeable payloads such as MMAF.(37) Initial co-culture experiments of CD25-negative Ramos with CD25-positive Karpas 299 resulted in loss of Ramos cells, possibly due to the Treg suppressive phenotype of Karpas 299.(38) Therefore, Ramos and Karpas 299 were co-cultured in the presence of a TGF-β signalling antagonist to ablate the T-reg suppressive effect.(39) In both medium transfer and co-culture experiments, Ramos cells were killed by a soluble factor released from ADCT-301-treated Karpas 299 cells into the medium. We hypothesise that this soluble factor is SG3199 warhead, released by lysosomal cleavage of the val-ala dipeptide linker in ADCT-301 and the self-immolative cleavage of the residual linker stub on the PBD N10 imine, since we have shown that any transfer of intact ADC would be inactive against the CD25-negative Ramos cells.

Evidence for internalization of ADCT-301 is provided both by the decline of detected ADC on the cell surface of Karpas 299 and the reduction in intensity of membrane immunofluorescent staining on L-540 cells. Furthermore, a reduction of CD25 surface expression over the first three hours after ADCT-301 treatment is evident, following which expression returns to pre-treatment levels by 16h. There is no binding competition between the two anti-CD25 antibodies used in this latter assay suggesting that the decline in the CD25 copy number represents internalization and downmodulation. Immunofluorescent co-localization images show that processing of ADCT-301 is at least in part lysosomal.

An important feature of the highly cytotoxic interstrand cross-linking produced by PBD dimer warheads is the minimal DNA distortion which may be responsible for a lack of repair of these cross-links and their persistence.(40, 41) The time lag between the peak of cross-

linking by ADCT-301 and by equimolar warhead likely reflects the slower time taken for ADC internalization and cellular processing compared with the diffusible active warhead. We detected no cross-link repair over 36h. The strong correlation between the reduction in OTM and the loss of cell survival indicates that DNA cross-linking is an important mode of action of ADCT-301.

A DNA damage response (increased γ-H2AX foci) is evident in CD25-positive cells 24h after a two-hour exposure to ADCT-301 at concentrations as low as 60 pg/ml. This supports previous observations that γ-H2AX is highly sensitive to cellular events induced by DNA cross-linking agents including PBD dimers.(34, 41) DNA cross-linking leads to G2/M cell cycle arrest and apoptotic cell death.(40, 42) We have shown that ADCT-301 caused G2/M arrest peaking at 48h and apoptotic cell death. Thus we confirm that DNA cross-linking peaked by four to eight hours and was followed by a γ-H2AX response by 24h. G2/M arrest ensued at 48h, phosphatidylserine and phosphatidyltyramine exposure at 72h and loss of cell viability at 96h.

The MTD, PK and stability of ADCT-301 was explored in non-tumor bearing SCID mice. These mice tolerated ADCT-301 up to 9 mg/kg. Measured half-lives of naked antibody and ADCT-301 in mice serum were identical. CD25 is constitutively expressed on Treg and on activated cytotoxic T lymphocytes, B lymphocytes (43) macrophages (44, 45) eosinophils (46) and basophils (47). Anti-CD25 immunoconjugates may contribute to the depletion of intratumoral CD25-expressing T cells including Tregs as has been demonstrated for ^{90}Yttrium-labeled daclizumab(18) and LMB-2 (48). Although the safety and efficacy of administering anti-CD25 radiommunoconjugates (16-18) and immunotoxins (19, 20) has been established in previous Phase I trials, the consequences of prolonged ablation of Tregs remains to be determined.

Mice xenografted with Karpas 299 and treated with ADCT-301 show remarkable dose-response improvements in survival. Single-dose ADCT-301 shows superiority to single-dose Adcetris administration in TTE statistical analyses despite the three-fold higher cell surface target expression for Adcetris and the higher DAR of Adcetris versus ADCT-301. Another CD25-expressing xenografted cell line, Su-DHL-1 showed significant dose-dependent delays in tumour growth and tumor-free survival after treatment with ADCT-301. The targeted *in vivo* efficacy of ADCT-301 is illustrated in the lack of efficacy in both non-targeted ADC treatment of Karpas 299 xenografts and in ADCT-301 treatment of a CD25-negative Ramos model.

Using a monoclonal anti-PBD antibody against a PBD payload and anti-γ-H2AX staining has confirmed the dose dependent delivery of ADC to the tumor xenograft. The comet assay and γ-H2AX immunofluorescence have been used as pharmacodynamics assays in previous clinical trials of PBD dimer, SG2000 (25, 26) and the comet assay was used to quantitatively assess DNA damage in excised tumor samples in the current study. Extrapolating from *in vivo* data, the mean reduction in OTM in 0.6 mg/kg-treated tumor cells compared to the 0.2 mg/kg cohort, suggests that a threshold level of DNA cross-linking may be required for *in vivo* efficacy. The absence of significant DNA cross-linking in SCID mouse PBMCs (CD25-negative) supports the CD25-specificity of ADCT-301 *in vivo*. These comet data thus provide a relevant pharmacodynamic assay for use in the current clinical development of PBD-based ADCs including ADCT-301.

Acknowledgments

The authors thank Charles River Laboratory Services for conducting the majority of the *in vivo* efficacy studies. Much appreciation is extended to members of other departments at UCL including GCLP staff, Janet Hartley and Victoria Spanswick for sharing their expertise (comet assay and γ-H2AX immunofluorescence), staff of the Biological Services Unit, Mathew Robson and Barbara Pedley for their assistance and guidance in conducting

additional *in vivo* experiments, and Vishvesh Shende and Joseph Linares from the Pathology Department for their help in setting up IHC assays. Other laboratory staff at Spirogen and ADCT in both chemistry and biology departments must be acknowledged for their guidance in setting up assays used in this project.

References

1. Siegel RL, Miller KD, Jemal A. Cancer statistics, 2015. CA Cancer J Clin. 2015;65:5-29.
2. Strauchen JA, Breakstone BA. IL-2 receptor expression in human lymphoid lesions. Immunohistochemical study of 166 cases. Am J Pathol. 1987;126:506-12.
3. Sheibani K, Winberg CD, van de Velde S, Blayney DW, Rappaport H. Distribution of lymphocytes with interleukin-2 receptors (TAC antigens) in reactive lymphoproliferative processes, Hodgkin's disease, and non-Hodgkin's lymphomas. An immunohistologic study of 300 cases. Am J Pathol. 1987;127:27-37.
4. Dasanu CA. Newer developments in adult T-cell leukemia/lymphoma therapeutics. Expert Opin Pharmacother. 2011;12:1709-17.
5. Shao H, Calvo KR, Gronborg M, Tembhare PR, Kreitman RJ, Stetler-Stevenson M, et al. Distinguishing hairy cell leukemia variant from hairy cell leukemia: development and validation of diagnostic criteria. Leuk Res. 2013;37:401-9.
6. Guo Z, Wang A, Zhang W, Levit M, Gao Q, Barberis C, et al. PIM inhibitors target CD25-positive AML cells through concomitant suppression of STAT5 activation and degradation of MYC oncogene. Blood. 2014;124:1777-89.
7. Srivastava MD, Srivastava A, Srivastava BI. Soluble interleukin-2 receptor, soluble CD8 and soluble intercellular adhesion molecule-1 levels in hematologic malignancies. Leuk Lymphoma. 1994;12:241-51.
8. Raziuddin S, Sheikha A, Abu-Eshy S, al-Janadi M. Circulating levels of cytokines and soluble cytokine receptors in various T-cell malignancies. Cancer. 1994;73:2426-31.
9. Yamauchi T, Matsuda Y, Takai M, Tasaki T, Tai K, Hosono N, et al. Early relapse is associated with high serum soluble interleukin-2 receptor after the sixth cycle of R-CHOP chemotherapy in patients with advanced diffuse large B-cell lymphoma. Anticancer Res. 2012;32:5051-7.
10. Kadin ME, Pavlov IY, Delgado JC, Vonderheid EC. High soluble CD30, CD25, and IL-6 may identify patients with worse survival in CD30+ cutaneous lymphomas and early mycosis fungoides. J Invest Dermatol. 2012;132:703-10.
11. Nakase K, Kita K, Kyo T, Tsuji K, Katayama N. High serum levels of soluble interleukin-2 receptor in acute myeloid leukemia: correlation with poor prognosis and CD4 expression on blast cells. Cancer Epidemiol. 2012;36:e306-9.
12. Yang ZZ, Grote DM, Ziesmer SC, Manske MK, Witzig TE, Novak AJ, et al. Soluble IL-2Ralpha facilitates IL-2-mediated immune responses and predicts reduced survival in follicular B-cell non-Hodgkin lymphoma. Blood. 2011;118:2809-20.
13. Pui CH, Ip SH, Kung P, Dodge RK, Berard CW, Crist WM, et al. High serum interleukin-2 receptor levels are related to advanced disease and a poor outcome in childhood non-Hodgkin's lymphoma. Blood. 1987;70:624-8.
14. Ambrosetti A, Nadali G, Vinante F, Carlini S, Veneri D, Todeschini G, et al. Serum levels of soluble interleukin-2 receptor in Hodgkin disease. Relationship with clinical stage, tumor burden, and treatment outcome. Cancer. 1993;72:201-6.

15. Katsuya H, Yamanaka T, Ishitsuka K, Utsunomiya A, Sasaki H, Hanada S, et al. Prognostic index for acute- and lymphoma-type adult T-cell leukemia/lymphoma. J Clin Oncol. 2012;30:1635-40.
16. Waldmann TA, White JD, Carrasquillo JA, Reynolds JC, Paik CH, Gansow OA, et al. Radioimmunotherapy of interleukin-2R alpha-expressing adult T-cell leukemia with Yttrium-90-labeled anti-Tac. Blood. 1995;86:4063-75.
17. Dancey G, Violet J, Malaroda A, Green AJ, Sharma SK, Francis R, et al. A Phase I Clinical Trial of CHT-25 a 131I-Labeled Chimeric Anti-CD25 Antibody Showing Efficacy in Patients with Refractory Lymphoma. Clin Cancer Res. 2009;15:7701-10.
18. Janik JE, Morris JC, O'Mahony D, Pittaluga S, Jaffe ES, Redon CE, et al. 90Y-daclizumab, an anti-CD25 monoclonal antibody, provided responses in 50% of patients with relapsed Hodgkin's lymphoma. Proc Natl Acad Sci U S A. 2015;112:13045-50.
19. Kreitman RJ, Wilson WH, White JD, Stetler-Stevenson M, Jaffe ES, Giardina S, et al. Phase I trial of recombinant immunotoxin anti-Tac(Fv)-PE38 (LMB-2) in patients with hematologic malignancies. J Clin Oncol. 2000;18:1622-36.
20. Kreitman RJ, Stetler-Stevenson M, Jaffe ES, Conlon KC, Steinberg SM, Wilson WH, et al. Complete remissions of adult T-cell leukemia with anti-CD25 recombinant immunotoxin LMB-2 and chemotherapy to block immunogenicity. Clin Cancer Res. 2016;22:310-8
21. Olsen E, Duvic M, Frankel A, Kim Y, Martin A, Vonderheid E, et al. Pivotal phase III trial of two dose levels of denileukin diftitox for the treatment of cutaneous T-cell lymphoma. J Clin Oncol. 2001;19:376-88.
22. Madhumathi J, Devilakshmi S, Sridevi S, Verma RS. Immunotoxin therapy for hematologic malignancies: where are we heading? Drug Discov Today. 2016;21(2):325-32.
23. Wayne AS, Fitzgerald DJ, Kreitman RJ, Pastan I. Immunotoxins for leukemia. Blood. 2014;123:2470-7.
24. Adair JR, Howard PW, Hartley JA, Williams DG, Chester KA. Antibody-drug conjugates - a perfect synergy. Expert Opin Biol Ther. 2012;12:1191-206.
25. Puzanov I, Lee W, Chen AP, Calcutt MW, Hachey DL, Vermeulen WL, et al. Phase I pharmacokinetic and pharmacodynamic study of SJG-136, a novel DNA sequence selective minor groove cross-linking agent, in advanced solid tumors. Clin Cancer Res. 2011;17:3794-802.
26. Janjigian YY, Lee W, Kris MG, Miller VA, Krug LM, Azzoli CG, et al. A phase I trial of SJG-136 (NSC#694501) in advanced solid tumors. Cancer Chemother Pharmacol. 2010;65:833-8.
27. Kung Sutherland MS, Walter RB, Jeffrey SC, Burke PJ, Yu C, Kostner H, et al. SGN-CD33A: a novel CD33-targeting antibody-drug conjugate using a pyrrolobenzodiazepine dimer is active in models of drug-resistant AML. Blood. 2013;122:1455-63.
28. Tiberghien AC, Levy J-N, Masterson LA, Patel NV, Adams LR, Corbett S, et al. Design and Synthesis of Tesirine, a Clinical Antibody–Drug Conjugate Pyrrolobenzodiazepine Dimer Payload. ACS Medicinal Chemistry Letters. 2016.
29. DAKO. QIFIKIT® Code K0078: DK-2600 [Internet]. 2008. [cited 14 April 2014]. Available from: http://www.dako.com/uk/download.pdf?objectid=111993002
30. Riss TL, Moravec RA, Niles AL, Benink HA, Worzella TJ, Minor L, et al. Cell Viability Assays. In: Sittampalam GS, Coussens NP, Nelson H, Arkin M, Auld D, Austin C, et al., editors. Assay Guidance Manual. Bethesda (MD): Eli Lilly & Company and the National Center for Advancing Translational Sciences; 2004.
31. Spanswick VJ, Hartley JM, Hartley JA. Measurement of DNA interstrand crosslinking in individual cells using the Single Cell Gel Electrophoresis (Comet) assay. Methods Mol Biol. 2010;613:267-82.
32. Marafioti T, Jones M, Facchetti F, Diss TC, Du MQ, Isaacson PG, et al. Phenotype and genotype of interfollicular large B cells, a subpopulation of lymphocytes often with dendritic morphology. Blood. 2003;102:2868-76.
33. Marafioti T, Pozzobon M, Hansmann ML, Delsol G, Pileri SA, Mason DY. Expression of intracellular signaling molecules in classical and lymphocyte predominance Hodgkin disease. Blood. 2004;103:188-93.

34. Wu J, Clingen PH, Spanswick VJ, Mellinas-Gomez M, Meyer T, Puzanov I, et al. gamma-H2AX foci formation as a pharmacodynamic marker of DNA damage produced by DNA cross-linking agents: results from 2 phase I clinical trials of SJG-136 (SG2000). Clin Cancer Res. 2013;19:721-30.
35. Jeffrey SC, Burke PJ, Lyon RP, Meyer DW, Sussman D, Anderson M, et al. A potent anti-CD70 antibody-drug conjugate combining a dimeric pyrrolobenzodiazepine drug with site-specific conjugation technology. Bioconjug Chem. 2013;24:1256-63.
36. Saunders LR, Bankovich AJ, Anderson WC, Aujay MA, Bheddah S, Black K, et al. A DLL3-targeted antibody-drug conjugate eradicates high-grade pulmonary neuroendocrine tumor-initiating cells in vivo. Sci Transl Med. 2015;7:302ra136.
37. Doronina SO, Mendelsohn BA, Bovee TD, Cerveny CG, Alley SC, Meyer DL, et al. Enhanced activity of monomethylauristatin F through monoclonal antibody delivery: effects of linker technology on efficacy and toxicity. Bioconjug Chem. 2006;17:114-24.
38. Wolke C, Tadje J, Bukowska A, Tager M, Bank U, Ittenson A, et al. Assigning the phenotype of a natural regulatory T-cell to the human T-cell line, KARPAS-299. Int J Mol Med. 2006;17:275-8.
39. Kawabata KC, Ehata S, Komuro A, Takeuchi K, Miyazono K. TGF-beta-induced apoptosis of B-cell lymphoma Ramos cells through reduction of MS4A1/CD20. Oncogene. 2013;32:2096-106.
40. Hartley JA, Spanswick VJ, Brooks N, Clingen PH, McHugh PJ, Hochhauser D, et al. SJG-136 (NSC 694501), a novel rationally designed DNA minor groove interstrand cross-linking agent with potent and broad spectrum antitumor activity: part 1: cellular pharmacology, in vitro and initial in vivo antitumor activity. Cancer Res. 2004;64:6693-9.
41. Clingen PH, De Silva IU, McHugh PJ, Ghadessy FJ, Tilby MJ, Thurston DE, et al. The XPF-ERCC1 endonuclease and homologous recombination contribute to the repair of minor groove DNA interstrand crosslinks in mammalian cells produced by the pyrrolo[2,1-c][1,4]benzodiazepine dimer SJG-136. Nucleic Acids Res. 2005;33:3283-91.
42. Osawa T, Davies D, Hartley JA. Mechanism of cell death resulting from DNA interstrand cross-linking in mammalian cells. Cell Death Dis. 2011;2:e187.
43. Boyman O, Sprent J. The role of interleukin-2 during homeostasis and activation of the immune system. Nature reviews Immunology. 2012;12:180-90.
44. Holter W, Goldman CK, Casabo L, Nelson DL, Greene WC, Waldmann TA. Expression of functional IL 2 receptors by lipopolysaccharide and interferon-gamma stimulated human monocytes. J Immunol. 1987;138:2917-22.
45. Herrmann F, Cannistra SA, Levine H, Griffin JD. Expression of interleukin 2 receptors and binding of interleukin 2 by gamma interferon-induced human leukemic and normal monocytic cells. J Exp Med. 1985;162:1111-6.
46. Riedel D, Lindemann A, Brach M, Mertelsmann R, Herrmann F. Granulocyte-macrophage colony-stimulating factor and interleukin-3 induce surface expression of interleukin-2 receptor p55-chain and CD4 by human eosinophils. Immunology. 1990;70:258-61.
47. Maggiano N, Colotta F, Castellino F, Ricci R, Valitutti S, Larocca LM, et al. Interleukin-2 receptor expression in human mast cells and basophils. Int Arch Allergy Appl Immunol. 1990;91:8-14.
48. Powell DJ, Felipe-Silva A, Merino MJ, Ahmadzadeh M, Allen T, Levy C, et al. Administration of a CD25-Directed Immunotoxin, LMB-2, to Patients with Metastatic Melanoma Induces a Selective Partial Reduction in Regulatory T Cells In Vivo. The Journal of Immunology. 2007;179:4919-28.

Tables

Table 1. CD25-positive and negative cell lines were incubated with increasing concentrations of ADCT-301, or free warhead (SG3199) for 96 hours before processing by the MTS assay. Data for each cell line are presented as the GI_{50} i.e. 50% of the net tetrazolium reduction product increase in untreated cells. The mean number of CD25 molecules per cell line was determined by flow cytometric analysis using Qifikit (DAKO).

Cell line	Tumour type	Mean CD25 molecules per cell surface (thousands)	GI_{50}	
			ADCT-301 ng/ml (pM)	SG3199 (pM)
Su-DHL-1	ALCL	310	0.74 (4.96)	12.11
HDLM-2	HL	167	2.94 (19.60)	158.60
L-540	HL	96	1.11 (7.49)	14.80
Karpas 299	ALCL	77	2.56 (17.07)	18.49
Ramos	Burkitt's	< 1 *	> 1,000 (> 6,667)	5.83
Daudi	Burkitt's	< 1 *	> 1,000 (> 6,667)	18.11
HuT-78	CTCL	< 1 *	> 1,000 (> 6,667)	12.98
EoL-1	AML	17	0.04 (0.26)	0.79
KG-1	AML	< 1 *	> 1,000 (> 6,667)	[Y]ND

* 1,000 reflects the limits of sensitivity of this assay below which cell lines were considered CD25 negative. [Y] not determined

Figure Legends

Figure 1

A. Structure of ADCT-301

B. Flow cytometry measurement of median fluorescent intensity showing binding of ADCT-301, HuMax-TAC, and non-binding ADC binding to Karpas 299 and Su-DHL-1 CD25-positive human cell lines.

C. Biacore® sensogram depicting injections of naked antibody, HuMax-TAC over a Biacore CM3 chip which had soluble CD25 ectodomain immobilized onto its surface. Arrow indicates the end of the ADC injection and the beginning of the dissociation run.

D. Corresponding sensogram for ADCT-301

Figure 2

A. Histograms depicting percentage viable CD25-negative Ramos cells in mono-culture (black bar) and Ramos+Karpas 299 (white bar) in co-culture (50:50) treated with 1 or 10 ng/ml of either ADCT-301 (top) (*** $p \leq 0.001$) or non-binding ADC (bottom) for 96 hours (ns = not significant).

B. Viability curves showing percentage Ramos viability compared to untreated control wells after a 96 hour exposure either to ADC (black square) or to media transferred from ADC-treated Karpas 299 (white triangle). The original ADCT-301 concentration titration series is plotted in the top panel ($p \leq 0.05$) and that of the non-binding ADC in the bottom panel (not significant).

C. Merged immunofluorescence images of CD25-positive L-540 cells treated with ADCT-301 (1 µg/ml) for 1 hour, washed and fixed after T=0, 1 or 4 hours in medium at 37 °C and stained with labeled anti-human IgG (green), anti-LAMP-1 (red) and

Hoechst 33342 (blue) nuclear stain. Yellow indicates co-localization. Non-binding ADC-treated L-540 cells are shown at T=0.

D. Line graph showing the mean CD25 molecules per cell present on the surface of ADCT-301 treated (1 µg/ml) Karpas 299 cells over a time course to 16 hours as a percentage of the mean CD25 molecules per cell present on untreated Karpas 299

E. Line graphs depicting median fluorescence of cells incubated at 37°C in medium versus cells kept at 4°C in 0.1% sodium azide at 1, 2 and 4 hours after ADCT-301 treatment.

Figure 3

A. The single cell-gel electrophoresis (comet) assay was carried out on untreated irradiated or un-irradiated Karpas 299 and 1 or 15 ng/ml ADCT-301 or non-binding ADC -treated irradiated cells, with image panels showing DNA labeled with propidium iodide for each treatment condition.

B. Line graph showing the percentage reduction in OTM compared to untreated control in Karpas 299 cells treated with 300 pM naked warhead, 20 ng/ml (133 pM) (ADCT-301 or non-binding ADC

C. Percentage reduction in OTM in Su-DHL-1 cells treated with 300 pM naked warhead or 20 ng/ml (133 pM) ADCT-301

D. Percentage viability and percentage reduction in OTM are plotted versus concentration of equivalent warhead in ADCT-301 treated Karpas 299.

E. The equivalent curves are plotted for ADCT-301 treated Su-DHL-1.

Figure 4

A. Image panels depict Karpas 299 cells untreated, or treated with 60 pg/ml or 1 ng/ml ADCT-301 and then stained with AF-488-labeled anti-γ-H2AX (first column) or

Hoechst 33342 nuclear stain (middle column). The third column shows the image overlays in color. Scale bars represent 20 μm. The bar chart (right) shows the mean fold increase in foci per cell in three independent experiments at each concentration compared to foci per untreated cell. (* = $p \leq 0.05$ ** $p \leq 0.01$).

B. Cell histograms of Karpas 299 either untreated, or treated with 10 ng/ml of non-binding ADC, 3 or 10 ng/ml of ADCT-301 for 48 hours, in each cell cycle phase (G1, S or G2/M) as determined by intensity of propidium iodide staining in one representative experiment. The bar chart (below) shows the percentage of cells in each cell cycle phase in three independent experiments for each of these treatment conditions. (* = $p \leq 0.05$)

C. Bar chart showing mean fold increase of cells in G2 phase compared to untreated control for cells treated with 3 ng/ml (20 pM) ADCT-301 or 15 pM naked warhead at 16, 24 or 48 hours.

D. Line graph showing percentage of Karpas 299 cells per well with surface Annexin V exposure or non-viable cells as indicated by permeability to viability dye over a time course (24, 48, 60, 72 and 96 hours) after treatment with 10 ng/ml ADCT-301 or non-binding ADC.

Figure 5

A. *In vivo* anti-tumor efficacy of ADCT-301 in subcutaneously implanted Karpas 299 xenograft model. Compared to injection of vehicle (PBS), ADCT-301 administered intravenously (i.v.) at a mean tumor volume of 160 mm^3 as a single dose at 0.1, 0.2, 0.4, and 0.6 mg/kg showed dose-dependent anti-tumor activity.

B. *In vivo* anti-tumor efficacy of ADCT-301 in comparison to Adcetris and Non-binding ADC. Vehicle (PBS), non-binding ADC (DAR 2.1), ADCT-301 (DAR 2.2) or Adcetris (DAR ~4) were administered i.v. at a mean Karpas 299 tumor volume of 130 mm^3 as

single doses at 0.5 mg/kg. Adcetris was also tested q4d x 4 at 0.5 mg/kg. The mean number of CD25 and CD30 molecules per Karpas 299 cell as determined by the flow cytometric Qifikit (DAKO) is shown in the inset to the graph.

C. *In vivo* anti-tumor efficacy of ADCT-301 in subcutaneously implanted Su-DHL-1 xenograft model. ADCT-301 was administered i.v. at mean tumor volume of 155 mm^3 at single doses of 0.3 mg/kg or 0.6 mg/kg and tumour growth compared to that observed after injection of vehicle (PBS).

D. Representative scans of formalin fixed paraffin embedded Karpas 299 tumor sections, obtained from untreated control SCID mice or mice treated with 0.2 and 0.6 mg/kg ADCT-301 and stained with an anti-PBD linker antibody (top panel) or an anti-γ-H2AX antibody (bottom panel). Scale bars indicate 100 μm. A magnified area of the anti-PBD linker antibody staining of tumors excised from animals dosed at 0.6 mg/kg is shown in the inset to this figure.

E. Histogram depicting mean OTM in irradiated tumor cell suspensions taken from Karpas 299 xenograft models untreated or 24 hours after injection with 0.2 mg/kg or 0.6mg/kg ADCT-301. (** = $p \leq 0.01$ *** $p \leq 0.001$)

Fig 1

A

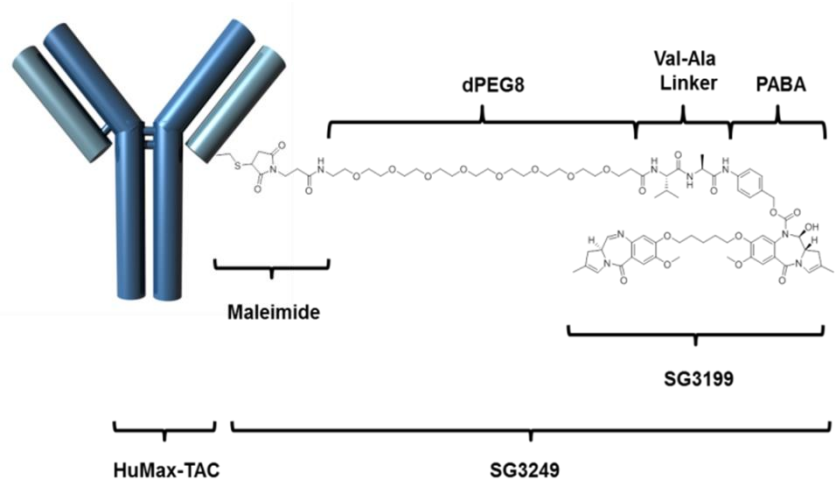
dPEG8
Val-Ala Linker
PABA
Maleimide
SG3199
HuMax-TAC
SG3249

B

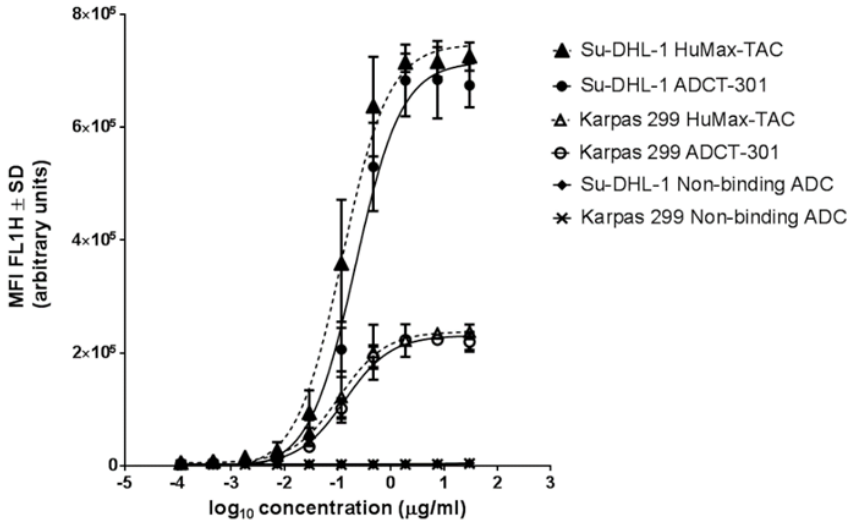
MFI FL1H ± SD (arbitrary units)
log10 concentration (µg/ml)
Su-DHL-1 HuMax-TAC
Su-DHL-1 ADCT-301
Karpas 299 HuMax-TAC
Karpas 299 ADCT-301
Su-DHL-1 Non-binding ADC
Karpas 299 Non-binding ADC

C

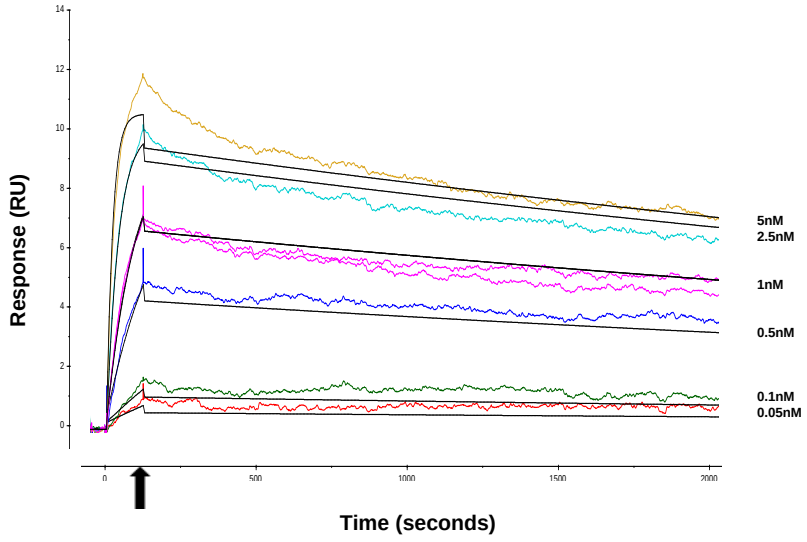
Response (RU)
Time (seconds)
5nM
2.5nM
1nM
0.5nM
0.1nM
0.05nM

D

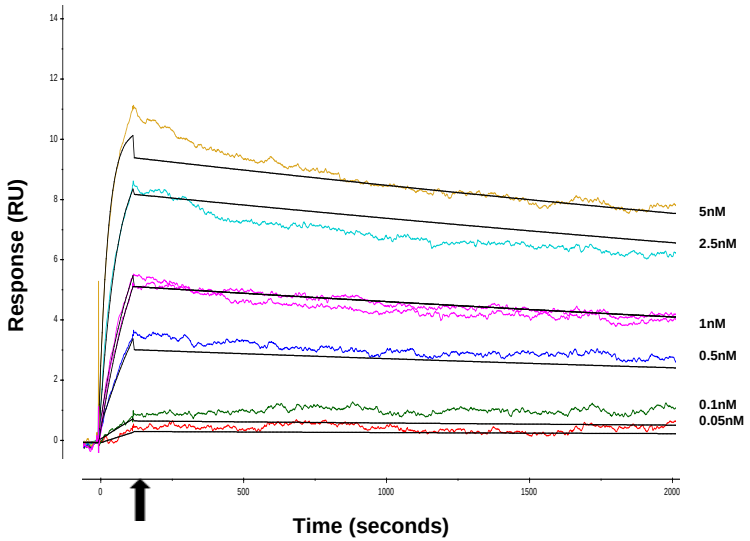
Response (RU)
Time (seconds)
5nM
2.5nM
1nM
0.5nM
0.1nM
0.05nM

Fig 2

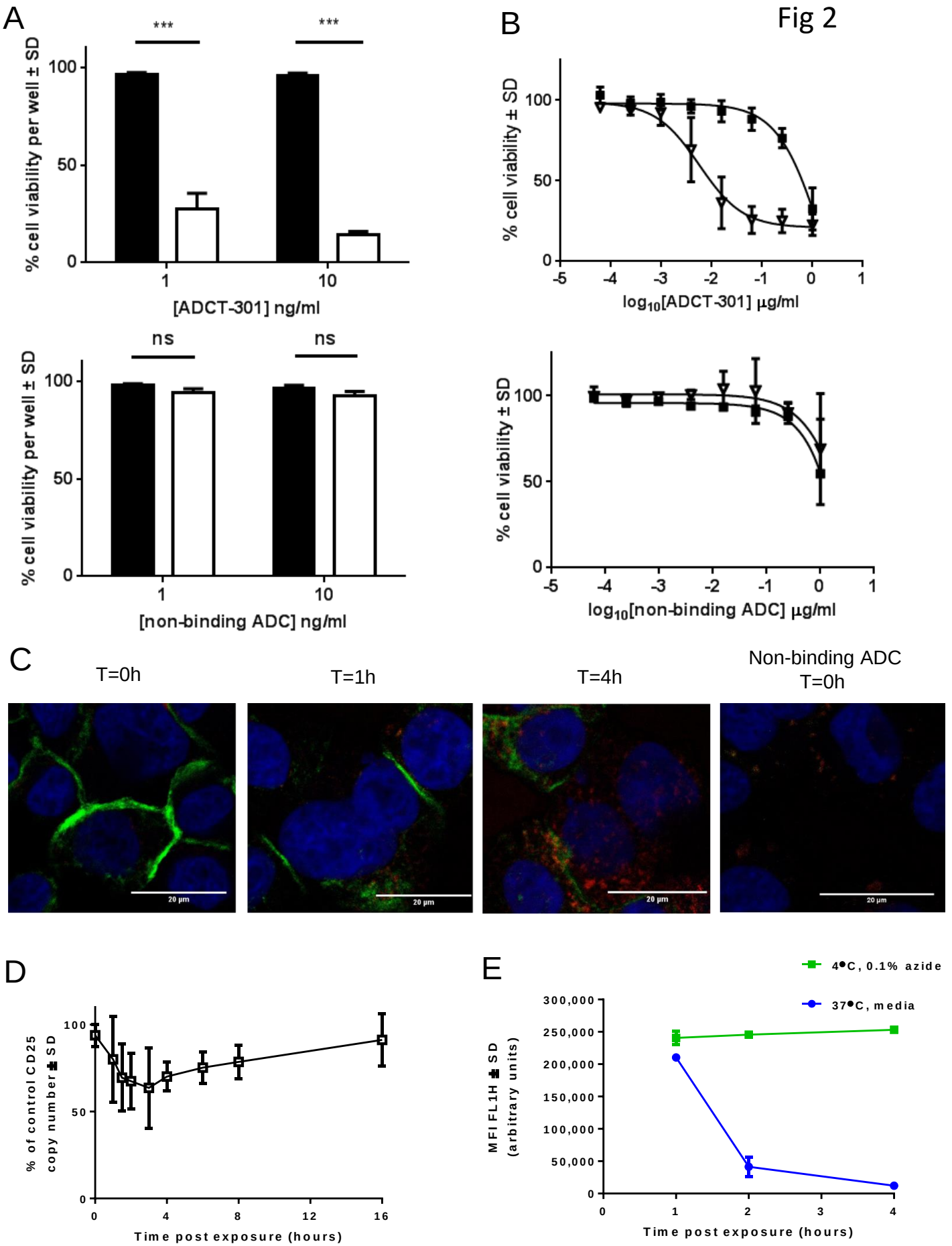
A
***
***
% cell viability per well ± SD
100
50
0
1
10
[ADCT-301] ng/ml
ns
ns
% cell viability per well ± SD
100
50
0
1
10
[non-binding ADC] ng/ml
B
% cell viability ± SD
100
50
0
-5
-4
-3
-2
-1
0
1
log10[ADCT-301] µg/ml
% cell viability ± SD
100
50
0
-5
-4
-3
-2
-1
0
1
log10[non-binding ADC] µg/ml
C
T=0h
T=1h
T=4h
Non-binding ADC
T=0h
20 µm
20 µm
20 µm
20 µm
D
% of control CD25
copy number ± SD
100
50
0
0
4
8
12
16
Time post exposure (hours)
E
4°C, 0.1% azide
37°C, media
MFI FL1H ± SD
(arbitrary units)
300,000
250,000
200,000
150,000
100,000
50,000
0
0
1
2
3
4
Time post exposure (hours)

Fig 3

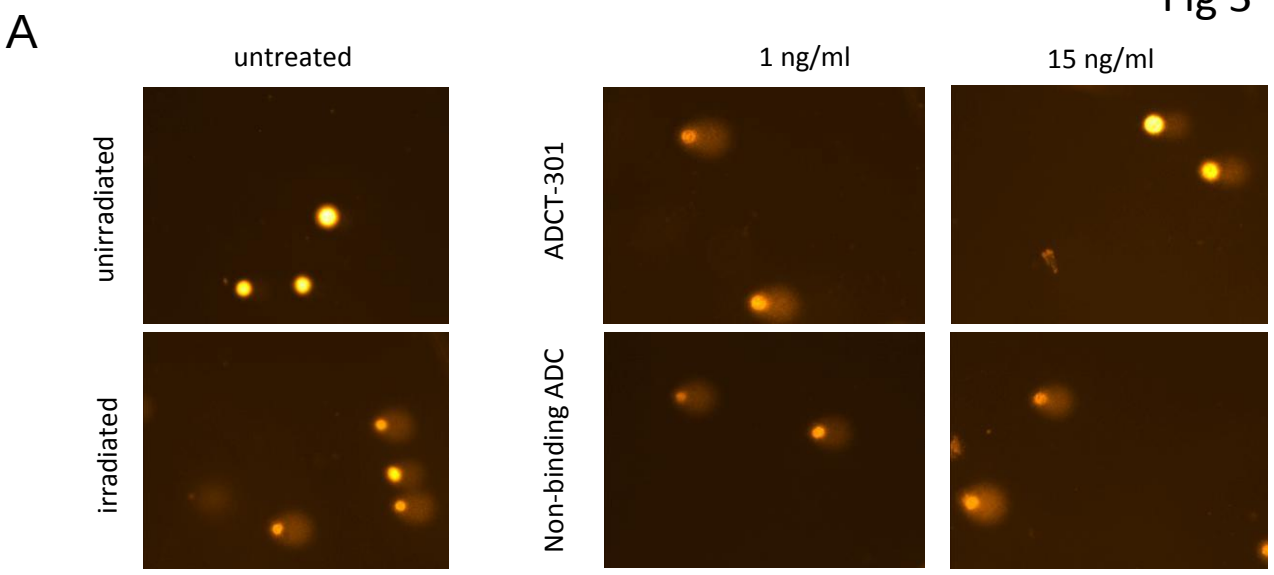
A
untreated
1 ng/ml
15 ng/ml
unirradiated
irradiated
ADCT-301
Non-binding ADC

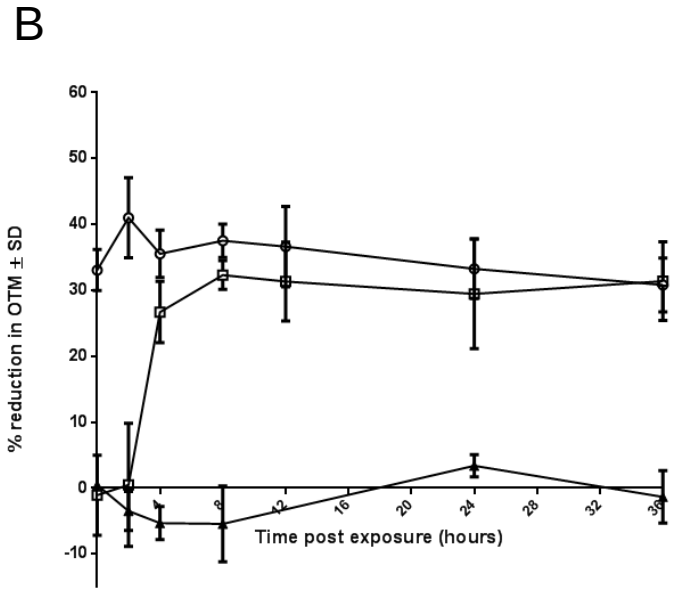
B
% reduction in OTM ± SD
Time post exposure (hours)

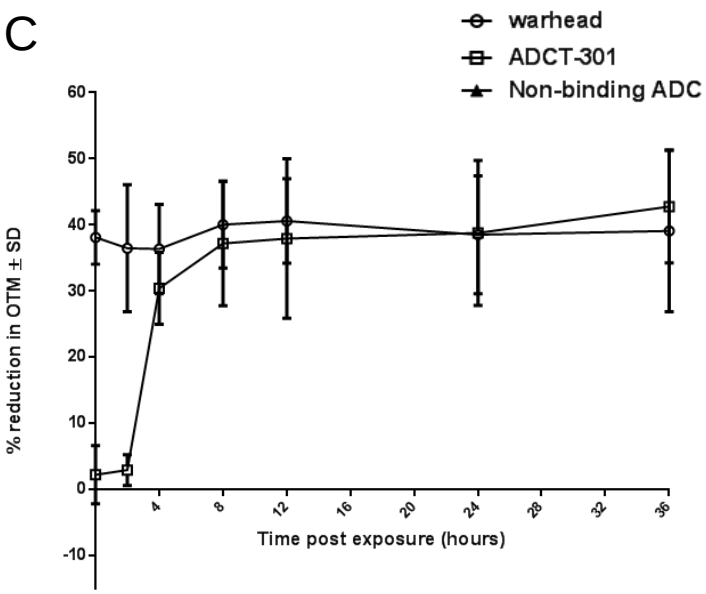
C
warhead
ADCT-301
Non-binding ADC
% reduction in OTM ± SD
Time post exposure (hours)

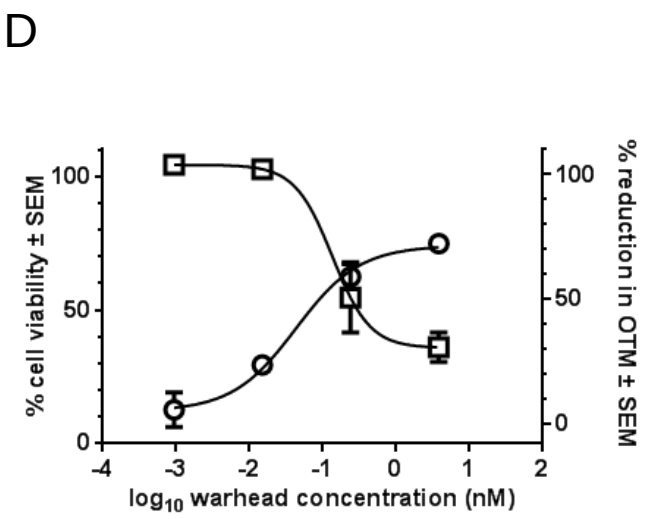
D
% cell viability ± SEM
% reduction in OTM ± SEM
log10 warhead concentration (nM)

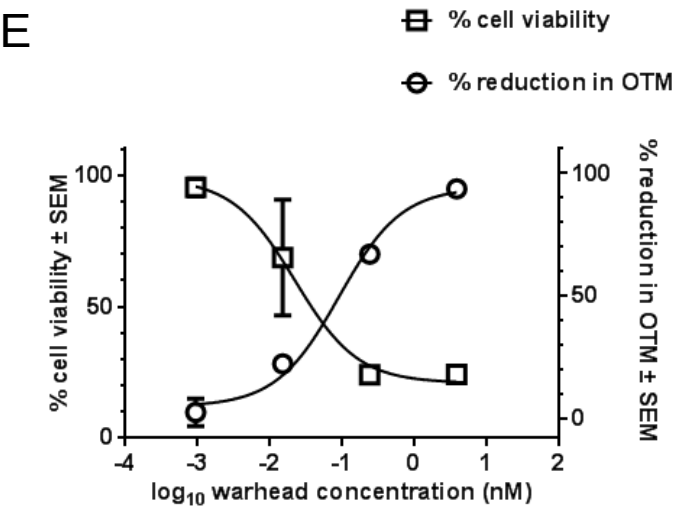
E
% cell viability
% reduction in OTM
% cell viability ± SEM
% reduction in OTM ± SEM
log10 warhead concentration (nM)

Fig 4

A

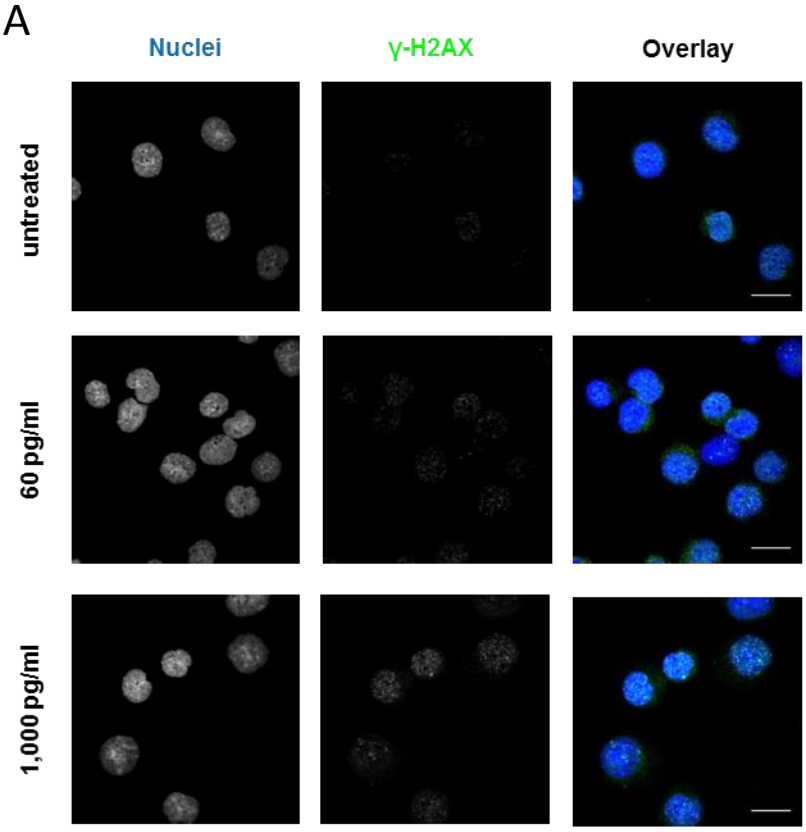
Nuclei
γ-H2AX
Overlay
untreated
60 pg/ml
1,000 pg/ml

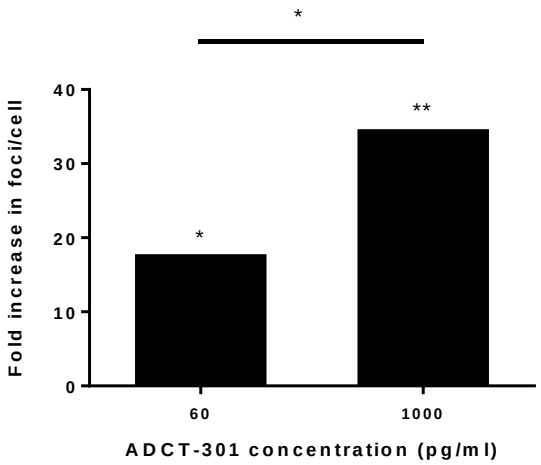
Fold increase in foci/cell
ADCT-301 concentration (pg/ml)
60
1000
*
**

B

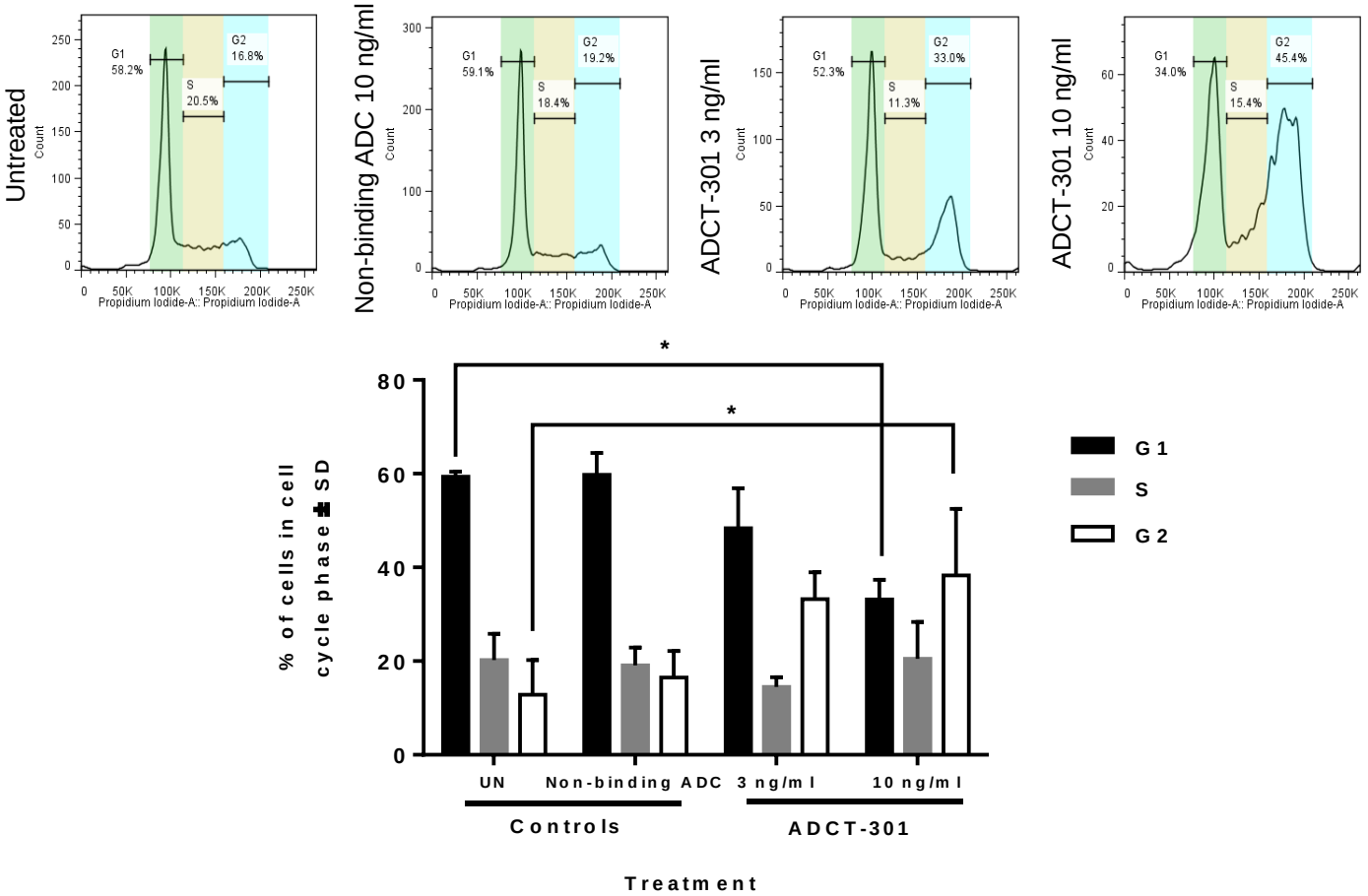
Untreated
Non-binding ADC 10 ng/ml
ADCT-301 3 ng/ml
ADCT-301 10 ng/ml
Propidium Iodide-A:: Propidium Iodide-A
% of cells in cell cycle phase ± SD
G1
S
G2
UN
Non-binding ADC
3 ng/ml
10 ng/ml
Controls
ADCT-301
Treatment

C

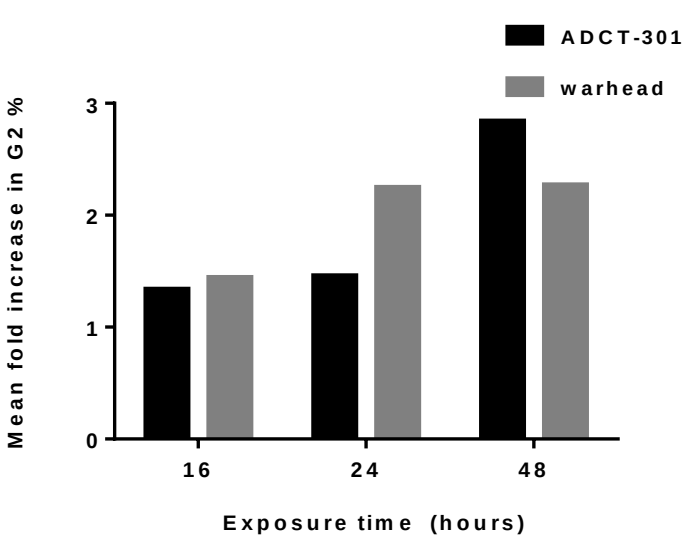
ADCT-301
warhead
Mean fold increase in G2 %
Exposure time (hours)

D

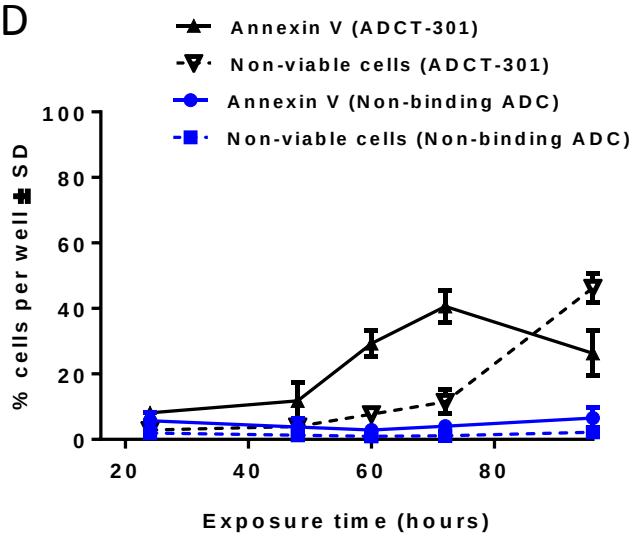
Annexin V (ADCT-301)
Non-viable cells (ADCT-301)
Annexin V (Non-binding ADC)
Non-viable cells (Non-binding ADC)
% cells per well ± SD
Exposure time (hours)

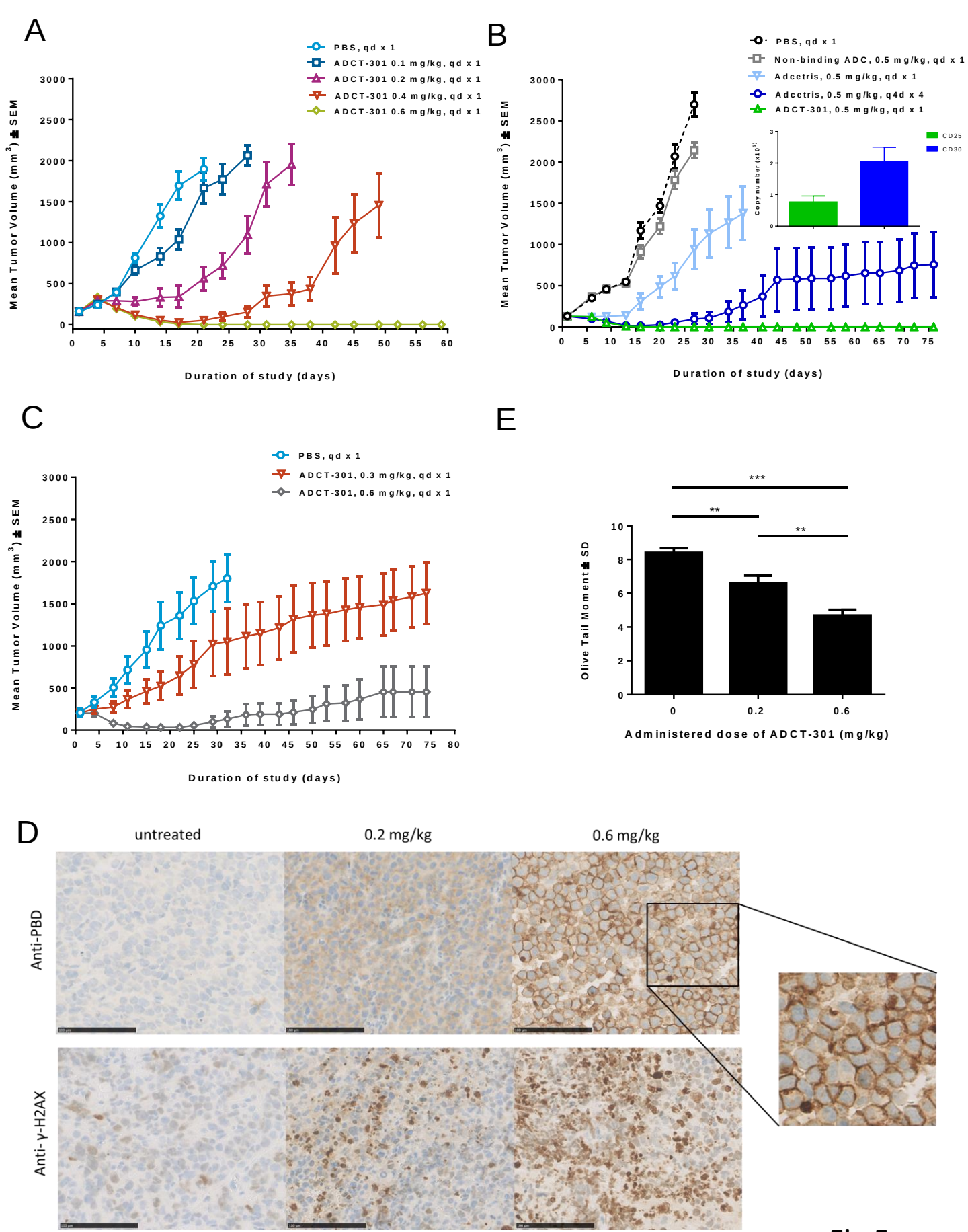
A
PBS, qd x 1
ADCT-301 0.1 mg/kg, qd x 1
ADCT-301 0.2 mg/kg, qd x 1
ADCT-301 0.4 mg/kg, qd x 1
ADCT-301 0.6 mg/kg, qd x 1
Mean Tumor Volume (mm3) ± SEM
Duration of study (days)
B
PBS, qd x 1
Non-binding ADC, 0.5 mg/kg, qd x 1
Adcetris, 0.5 mg/kg, qd x 1
Adcetris, 0.5 mg/kg, q4d x 4
ADCT-301, 0.5 mg/kg, qd x 1
CD25
CD30
Copy number (x10^5)
Mean Tumor Volume (mm3) ± SEM
Duration of study (days)
C
PBS, qd x 1
ADCT-301, 0.3 mg/kg, qd x 1
ADCT-301, 0.6 mg/kg, qd x 1
Mean Tumor Volume (mm3) ± SEM
Duration of study (days)
E
***
**
**
Olive Tail Moment ± SD
Administered dose of ADCT-301 (mg/kg)
D
untreated
0.2 mg/kg
0.6 mg/kg
Anti-PBD
Anti-γ-H2AX

Fig 5